AIP | Applied Physics Letters

Multiscale element mapping of buried structures by ptychographic x-ray diffraction microscopy using anomalous scattering

Yukio Takahashi, Akihiro Suzuki, Nobuyuki Zettsu, Yoshiki Kohmura, Kazuto Yamauchi et al.

Citation: Appl. Phys. Lett. **99**, 131905 (2011); doi: 10.1063/1.3644396
View online: http://dx.doi.org/10.1063/1.3644396
View Table of Contents: http://apl.aip.org/resource/1/APPLAB/v99/i13
Published by the American Institute of Physics.

Related Articles

Two-dimensional nanodiamond monolayers deposited by combined ultracentrifugation and electrophoresis techniques
Appl. Phys. Lett. 101, 253111 (2012)

The role of confinement on stress-driven grain boundary motion in nanocrystalline aluminum thin films
J. Appl. Phys. 112, 124313 (2012)

Luminescence properties of Sm3+ doped YPO4: Effect of solvent, heat-treatment, Ca2+/W6+-co-doping and its hyperthermia application
AIP Advances 2, 042184 (2012)

Site-controlled Ag nanocrystals grown by molecular beam epitaxy—Towards plasmonic integration technology
J. Appl. Phys. 112, 124302 (2012)

Surface-enhanced Raman scattering (SERS) based on copper vanadate nanoribbon substrate: A direct bio-detection without surface functionalization
J. Appl. Phys. 112, 114309 (2012)

Additional information on Appl. Phys. Lett.

Journal Homepage: http://apl.aip.org/
Journal Information: http://apl.aip.org/about/about_the_journal
Top downloads: http://apl.aip.org/features/most_downloaded
Information for Authors: http://apl.aip.org/authors

ADVERTISEMENT

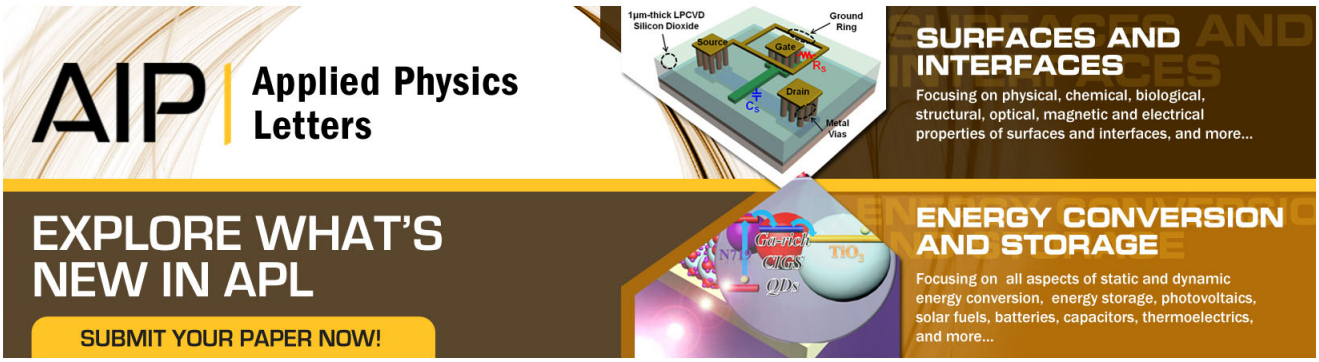

Multiscale element mapping of buried structures by ptychographic x-ray diffraction microscopy using anomalous scattering

Yukio Takahashi,[1,a)] Akihiro Suzuki,[1] Nobuyuki Zettsu,[2] Yoshiki Kohmura,[3] Kazuto Yamauchi,[1] and Tetsuya Ishikawa[3]
[1]*Department of Precision Science and Technology, Graduate School of Engineering, Osaka University, 2-1 Yamada-oka, Suita, Osaka 565-0871, Japan*
[2]*Department of Materials, Physics and Energy Engineering, Graduate School of Engineering, Nagoya University, Furocho, Chikusa-ku, Nagoya 464-8603, Japan*
[3]*RIKEN SPring-8 Center, 1-1-1 Kouto, Sayo-cho, Sayo, Hyogo 679-5148, Japan*

(Received 15 July 2011; accepted 6 September 2011; published online 28 September 2011)

We propose an element mapping technique of nano-meso-microscale structures buried within large and/or thick objects by ptychographic x-ray diffraction microscopy using anomalous scattering. We performed quantitative imagings of both the electron density and Au element of Au/Ag nanoparticles at the pixel resolution of better than 10 nm in a field of view larger than $5 \times 5\ \mu m^2$ by directly phasing ptychographic coherent diffraction patterns acquired at two x-ray energies below the Au L_3 edge. This method provides us with multiscale structural and elemental information for understanding the element/property relationship linking nanoscale structures to macroscopic functional properties in material and biological systems. © *2011 American Institute of Physics*. [doi:10.1063/1.3644396]

Advances in nanotechnology and nanoscience increasingly rely on characterization tools with various resolutions. Elemental information on heterogeneous structures in particular is crucial for diagnosing and predicting the properties of materials. Electron microscopy with electron energy-loss spectroscopy is a well-established technique that can be used to identify individual atoms in thin specimens.[1] Atom probe microscopy is also a powerful analytical tool, permitting the quantitative determination of material composition in a small selected region.[2] A now daunting task for these techniques is the nondestructive and elemental characterization of nano-meso-microscale structures buried within large and/or thick objects. This multiscale information is particularly important for understanding element/property relationship linking nanoscale structures to macroscopic functional properties, such as optical properties of arrayed nanoparticles,[3] mechanical properties of bulk nanostructured materials,[4] and neural networks connected with synapses.[5]

X-ray is a useful probe for obtaining elemental information on buried structures because of its high-penetration power and elemental identification at absorption edges. However, the spatial resolution of x-ray microscopy is still poor, which is currently limited by x-ray focusing optics. To overcome this obstacle, the lensless x-ray imaging technique based on coherent x-ray diffraction and phase retrieval calculation, which is called x-ray diffraction microscopy, has been developed[6] and applied to various material[7,8] and biological systems.[9] Element-specific diffraction microscopy has also been demonstrated using anomalous scattering around the absorption edge in the soft[10] and hard[11] x-ray regions. X-ray diffraction microscopy in the original concept, i.e., plane-wave diffraction microscopy, is limited to an object of finite size. Scanning x-ray diffraction microscopy, which is called x-ray ptychography, became a breakthrough that solved this limit.[12] Recently, high-resolution ptychography using focused x-ray beams[13,14] and biological applications in two[15,16] and three dimensions[17] have been reported.

In this letter, we report the demonstration of high-resolution element-specific ptychographic x-ray diffraction microscopy using anomalous scattering. We use high-intensity coherent x-ray beams produced by achromatic focusing optics. We present the high-resolution maps of both the electron density and target element of a sample in a large field of view.

Figure 1 shows a schematic of high-resolution element-specific ptychographic x-ray diffraction microscopy. Coherent diffraction patterns are collected so that the illumination area overlaps with the neighboring position. The complex transmission function of objects is iteratively retrieved using a ptychographical iterative engine,[18] which is well modeled using the projection approximation

$$T(x,y) = \exp\left(\frac{2\pi i}{\lambda}\int \delta(r) + i\beta(r)dz\right), \tag{1}$$

where λ is the wavelength, and δ and β are the phase and absorption terms of the refraction index, respectively. In the weak phase object approximation,[16] the transmission function can be written as

$$T(x,y) \approx 1 + \frac{2\pi i}{\lambda}\int \delta(r)dz. \tag{2}$$

If the object is composed of a single element, δ is expressed as $N\lambda^2 r_e(Z+f')/2\pi$, where Z is the electron number of an atom, f' is the real part of the anomalous dispersion terms, r_e is the classical electron radius, and N is the number of atoms per unit volume. By calculating the difference in T at two energies below the absorption edge of a specific element, the target element can be identified as the contrast of the difference in f' at the two energies.

a)Electronic mail: takahashi@prec.eng.osaka-u.ac.jp.

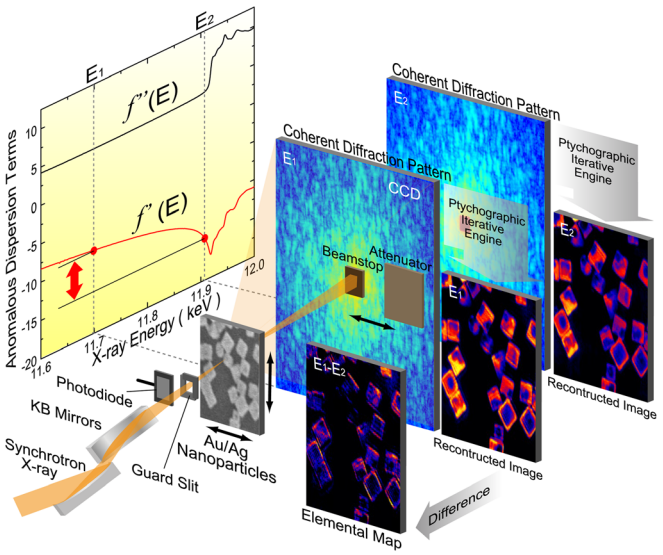

FIG. 1. (Color online) Schematic of the high-resolution element-specific x-ray ptychography. Scanning series of coherent diffraction patterns are collected at the two energies below the absorption edge of a specific element. The phase map of the sample is directly reconstructed using the ptychographic iterative engine. The difference in the two images represents the spatial distribution of the target element. In this study, Au/Ag nanoparticles were used as the sample. Two energies below the Au L_3 absorption edge were selected to identify the Au element of the nanoparticles. X-rays were highly focused using KB mirrors to collect diffraction data with a high S/N ratio.

Au/Ag nanoparticles[19] were used as the sample for the present demonstration experiment, which were mounted on a 100-nm-thick SiN membrane. The measurement of ptychographic x-ray diffraction patterns was carried out at BL29XUL (Ref. 20) in SPring-8. Incident x-rays were monochromatized at energies around the Au L_3 edge (11.920 keV) using a Si 111 double-crystal monochromator. The x-ray absorption spectrum of a 5-μm-thick Au foil around the Au L_3 edge was measured, and then the anomalous x-ray scattering factors were derived using the program CHOOCH (Ref. 21). The incident x-ray energies selected for coherent x-ray diffraction measurements were 11.700 and 11.910 keV, which were 220 and 10 eV below the Au L_3 edge, respectively. f' values of Au were calculated to be -9.16 for 11.700 keV and -14.96 for 11.910 keV, while theoretical f' values of Ag are -0.40 for 11.700 keV and -0.42 for 11.910 keV. To collect diffraction data with a high signal-to-noise (S/N) ratio, incident x-rays were focused to a spot size of $\sim$600 nm using a Kirkpatrick-Baez (KB) mirror pair that is convenient for multiple-energy experiments because of its achromatic property. The flux of the focused x-rays was estimated to be $\sim 3 \times 10^7$ photons/s. The sample was illuminated in 7×7 overlapping fields of view that were spaced by 500 nm. The data collection procedure is the same as that described in a previous report.[14] The x-ray exposure time of the in-vacuum front-illuminated charge-coupled device (CCD) detector at each position was 280 s. The total measurement time was $\sim$12 h for each energy.

The complex transmission function of the nanoparticles was reconstructed from the 49 diffraction patterns using the extended ptychographical iterative engine[22] within the weak phase object approximation.[16] The reconstruction was started from a flat object of unit transmission and an illumination wave field that was derived by x-ray ptychography of the known nanostructured sample. The iterative process was continued for up to 4×10^3 iterations. In the reconstructed images, the degradation of the spatial resolution due to the vibration and instability of the x-ray beam, optics and instrument was not observed, which indicates that the present experiment was performed by using a high-quality x-ray beam and in a very stable environment, in addition, the correction of positioning errors worked well.[14]

Figure 2(a) shows the reconstructed phase map of the complex transmission function of the nanoparticles with a pixel size of 8.4 nm. The weak phase object approximation is justified since the amount of phase shift is less than $\sim$0.30 rad. Approximately 450 nanoparticles and a single nanorod are clearly visible in the field of view larger than $5 \times 5\ \mu m^2$. Figure 2(b) shows the field-emission scanning electron microscopy (FE-SEM; HITACHI S-4800, 5 kV) image at the same region as that shown in Fig. 2(a). The positions of the individual particles correspond well in both images, which indicates that the focused x-rays were illuminated at the exact position on the sample and then highly reliable image reconstruction was performed. Only the surface of the particles can be observed in the FE-SEM image, while partially hollow interiors in the individual particles and partially nanotubes in the nanorod are clearly visible in the x-ray ptychography image. If one uses transmission electron microscopy, the hollow interiors can be observed.[8] However, the contrast at the frame is difficult to interpret because the multiple scattering and inelastic scattering of the electrons should be considerable. On the other hand, the x-ray ptychography has an advantage, that is, one is able to quantitatively evaluate the hollow interiors as the contrast of the electron density distribution. The phase shift of 0.1 rad in Fig. 2(a) corresponds to 3.4×10^5 electrons/nm^2.

Figures 3(a) and 3(b) show the phase maps in color scale at 11.700 and 11.910 keV, respectively, which correspond to the square area shown in Fig. 2(a). In both images, the shapes of individual particles are relatively similar, while the amount of phase shift of a part of the nanostructures is slightly different. Figure 3(c) shows the difference image between the phase maps at 11.700 and 11.910 keV, which is the Au elemental map of the nanoparticles. The Au-rich region exists on the surface of the particles, which is consistent with the existence of the wall made of Au-Ag alloys.[23] Figure 3(d) shows the cross-sectional plots of the wall of the

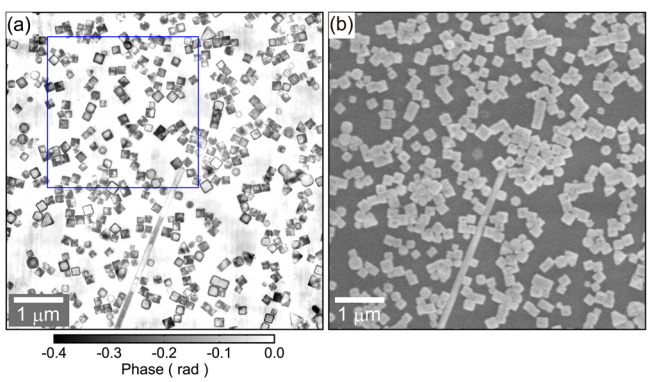

FIG. 2. (Color online) (a) Phase map of the Au/Ag nanoparticles reconstructed from the diffraction patterns at 11.7 keV. The pixel size is 8.4 nm. The total pixel size is 635×635. (b) FE-SEM image of the same area as the image of (a).

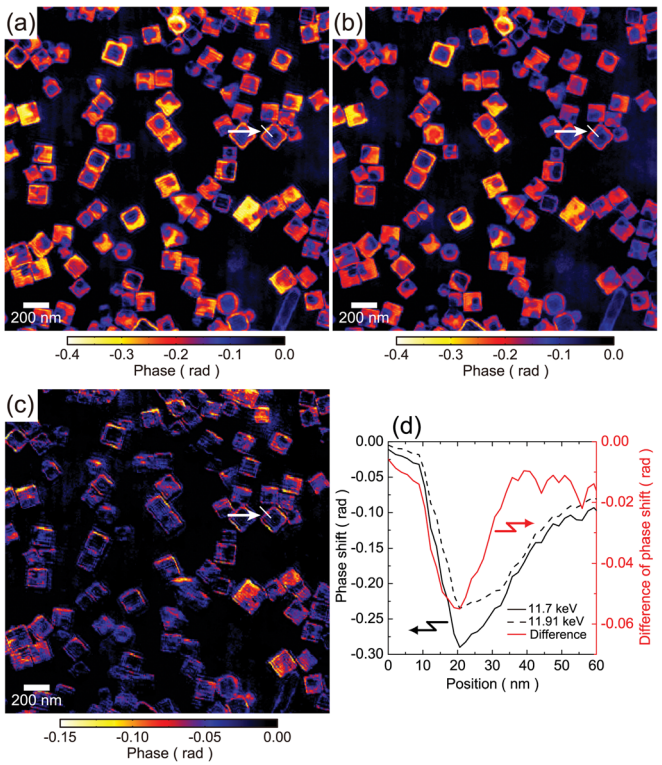

FIG. 3. (Color online) Reconstructed phase maps of the Au/Ag nanoparticles at (a) 11.7 keV and (b) 11.91 keV. The pixel size is 8.4 nm. The total pixel size is 300×300. The same area is indicated by the square shown in Fig. 2(a). (c) Difference image of the phase maps at 11.7 and 11.91 keV. (d) Cross sections through the white lines in (a)-(c).

particle through the white lines shown in the Figs. 3(a)–3(c). The full width at half maximum (FWHM) of the Au-rich wall is ~20 nm, which is about half of the FWHM of the wall. This implies that a pure Ag region exists inside the wall. The height of the Au region of the wall was estimated to be 220 nm from the difference in the phase shift, which is nearly equal to the edge length of the nanobox. Therefore, there is a possibility that the surface is covered with pure Au metal not with the Au-Ag alloy.

In conclusion, we have established high-resolution element-specific ptychographic x-ray diffraction microscopy using anomalous scattering around a specific element. We visualized Au-rich regions of individual particles of ~450 Au/Ag nanoparticles with sub-10 nm resolution in the field of view of more than $5 \times 5\ \mu m^2$. The present method provides us with multiscale structural and elemental informations for understanding the element/property relationship linking nanoscale structures to macroscopic functional properties in various material and biological systems. At present, both the actual spatial resolution and measurement time are limited by the flux density of coherent x-rays. In the near future, the high-resolution elemental mapping and the dynamics studies will be realized using high-brilliant coherent x-ray source such as x-ray free-electron lasers.

This work was supported by a Grant-in-Aid for Scientific Research (Grants Nos. 21686060, 22651040, and 23102504) and the Global COE Program "Center of Excellence for Atomically Controlled Fabrication Technology" from the Ministry of Education, Culture, Sports, Science and Technology.

[1]K. Suenaga, M. Tencé, C. Mory, C. Colliex, H. Kato, T. Okazaki, H. Shinohara, K. Hirahara, S. Bandow, and S. Iijima, Science **290**, 2280 (2000).
[2]D. Blavette, A. Bostel, J. M. Sarrau, B. Deconihout, and A. Menand, Nature (London) **363**, 432 (2000).
[3]H. A. Atwater and A. Polman, Nature Mater. **9**, 205 (2010).
[4]*Bulk Nanostructured Materials*, edited by M. J. Zehtbauer and Y. T. Zhu (Wiley-VCH, Weinheim, 2009).
[5]J. W. Lichtman and J. R. Sanes, Nat. Rev. Neurosci. **9**, 417 (2008).
[6]J. Miao, P. Charalambous, J. Kirz, and D. Sayre, Nature (London) **400**, 342 (1999); H. N. Chapman and K. A. Nugent, Nat. Photonics **30**, 833 (2010).
[7]M. A. Pfeifer, G. J. Williams, I. A. Vartanyants, R. Harder, and I. K. Robinson, Nature (London) **442**, 63 (2006); Y. Takahashi, Y. Nishino, T. Ishikawa, and E. Matsubara, Appl. Phys. Lett. **90**, 184105 (2007); B. Abbey, G. J. Williams, M. A. Pfeifer, J. N. Clark, C. T. Putkunz, A. Torrance, I. McNulty, T. M. Levin, A. G. Peele, and K. A Nugent, Appl. Phys. Lett. **93**, 214101 (2008).
[8]Y. Takahashi, N. Zettsu, Y. Nishino, R. Tsutsumi, E. Matsubara, T. Ishikawa, and K. Yamauchi, Nano Lett. **10**, 1922 (2010).
[9]J. Miao, K. O. Hodgson, T. Ishikawa, C. A. Larabell, M. A. LeGros, and Y. Nishino, Proc. Natl. Acad. Sci. U.S.A. **100**, 110 (2003); Y. Nishino, Y. Takahashi, N. Imamoto, T. Ishikawa, and K. Maeshima, Phys. Rev. Lett. **102**, 018101 (2009); J. Nelson, X. Huang, J. Steinbrener, D. Shapiro, J. Kirz, S. Marchesini, A. M. Neiman, J. J. Turner, and C. Jacobsen, Proc. Natl. Acad. Sci. U.S.A. **107**, 7235 (2010); H. Jiang, C. Song, C. C. Chen, R. Xu, K. S. Raines, B. P. Fahimian, C. H. Lu, T. K. Lee, A. Nakashima, J. Urano, T. Ishikawa, F. Tamanoi, and J. Miao, Proc. Natl. Acad. Sci. U.S.A. **107**, 11234 (2010); M. M. Seibert, T. Ekeberg, F. R. N. C. Maia, M. Svenda, J. Andreasson, O. Jönsson, D. Odić, B. Iwan, A. Rocker, D. Westphal, *et al.*, Nature (London) **470**, 78 (2011).
[10]C. Song, R. Bergstrom, D. Ramunno-Johnson, H. Jiang, D. Paterson, M. D. de Jonge, I. McNulty, J. Lee, K. L. Wang, and J. Miao, Phys. Rev. Lett. **100**, 025504 (2008); A. Scherz, D. Zhu, R. Rick, W. F. Schlotter, S. Roy, J. Lüning, and J. Stöhr, Phys. Rev. Lett. **101**, 076101 (2008).
[11]Y. Takahashi, H. Kubo, H. Furukawa, K. Yamauchi, E. Matsubara, T. Ishikawa, and Y. Nishino, Phys. Rev. B **78**, 092105 (2008).
[12]J. M. Rodenburg, A. C. Hurst, A. G. Cullis, B. R. Dobson, F. Pfeiffer, O. Bunk, C. David, K. Jefimovs, and I. Johnson, Phys. Rev. Lett. **98**, 034801 (2007).
[13]P. Thibault, M. Dierolf, A. Menzel, O. Bunk, C. David, and F. Pfeiffer, Science **321**, 321 (2008); A. Schropp, P. Boye, J. M. Feldkamp, R. Hoppe, J. Patommel, D. Samberg, S. Stephan, K. Giewekemeyer, R. N. Wilke, T. Salditt, J. Gulden, A. P. Mancuso, I. A. Vartanyants, E. Weckert, S. Schöder, M. Burghammer, and C. G. Schroer, Appl. Phys. Lett. **96**, 091102 (2010).
[14]Y. Takahashi, A. Suzuki, N. Zettsu, Y. Kohmura, Y. Senba, H. Ohashi, K. Yamauchi, and T. Ishikawa, Phys. Rev. B **83**, 214109 (2011).
[15]K. Giewekemeyer, P. Thibault, S. Kalbfleisch, A. Beerlink, C. M. Kewish, M. Dierolf, F. Pfeiffer, and T. Salditt, Proc. Natl. Acad. Sci. U.S.A. **107**, 529 (2009).
[16]M. Dierolf, P. Thibault, A. Menzel, C. M Kewish, K. Jefimovs, I. Schlichting, K. König, O. Bunk, and F. Pfeiffer, New. J. Phys. **12**, 035017 (2010).
[17]M. Dierolf, A. Menzel, P. Thibault, P. Schneider, C. M Kewish, R. Wepf, O. Bunk, and F. Pfeiffer, Nature (London) **467**, 436 (2010).
[18]H. M. L. Faulkner and J. M. Rodenburg, Phys. Rev. Lett. **93**, 023903 (2004).
[19]L. Au, X. Lu, and Y. Xia, Adv. Mater. **20**, 2517 (2008).
[20]K. Tamasaku, Y. Tanaka, M. Yabashi, H. Yamazaki, N. Kawamura, M. Suzuki, and T. Ishikawa, Nucl. Instrum. Methods Phys. Res. A **467–468**, 686 (2001).
[21]G. Evans and R. F. Pettifer, Acta Cryst. **A50**, 686 (1994).
[22]A. M. Maiden and J. M. Rodenburg, Ultramicroscopy **109**, 1256 (2009).
[23]Y. Sun and Y. Xia, J. Am. Chem. Soc. **126**, 3892 (2004).